Final Report for grant DE-SC0016084
Macro-physical Properties of Shallow Cumulus from Integrated ARM Observations

Submitted 10/27/2020
Report number DOE-LC-16084

J. M. Kleiss, Lewis & Clark college (Principal Investigator)
E. Kassianov, PNNL (Co-Investigator)
L. D. Riihimaki, Univ. of Colorado Boulder (Co-Investigator)
C. N. Long, Univ. of Colorado Boulder (Co-Investigator)
L. K. Berg, PNNL (Co-Investigator)

Abstract

Fair-weather shallow cumuli (ShCu) play an important role in many climate-related processes. Irregular geometry of ShCu and their strong temporal and spatial variability make it challenging to observe ShCu holistically and to represent them correctly in climate models. To improve ShCu parameterizations, information on both vertically and horizontally resolved cloud properties is required. Commonly, the vertically resolved cloud properties are provided by zenith pointing lidar-radar observations with a very narrow field of view (FOV). Thus, these "pencil-beam" properties may not be representative of a larger surrounding area. Limited number of areal-averaged cloud properties, such as fractional sky cover (FSC), are offered typically by wide-FOV observations.

The main goal of our project was to integrate advantages of the narrow-FOV (vertical structure of clouds) and wide-FOV (spatial arrangement of clouds) observations for an improved characterization of single-layer ShCu observed at the Atmospheric Radiation Measurement (ARM) Southern Great Plains (SGP) site for an 18-yr period (2000-2017). There are four major accomplishments of our project:

- First, an updated operational cloud classification for days with ShCu has been suggested and evaluated through a detailed comparison with the manually curated records. Our classification extends successfully the latest ARM cloud type Value Added Product (VAP) based on the Active Remote Sensing of Clouds (ARSCL) cloud product by incorporating both cloud fraction (CF) provided by narrow-FOV ceilometer data and FSC from wide-FOV images offered by a Total Sky Imager (TSI). Moreover, our classification allows one to identify impact of instrumentation changes at the SGP site, namely the transition to KAZRARSCL with the updated cloud radar, on the identification of periods with single-layer ShCu.
- Second, a new approach that resolves cloud area distributions for a given region (up to 4x4 km^2) has been suggested and cloud equivalent diameters (CEDs) have been estimated for the first time. These estimations have been performed over a wide range of cloud sizes (about 0.01–3.5 km) with high temporal resolution (30s) using wide-FOV TSI images and cloud base height (CBH) provided by complementary narrow-FOV lidar measurements. Our simple and computationally inexpensive approach offers a previously unavailable dataset for process studies in the convective boundary layer and evaluation of ShCu parameterizations in cloud-resolving models.
- Third, a long-term integrated record of ShCu macrophysical properties has been developed. The developed record represents the longest available compilation of events with ShCu and includes (i) a novel visualization of the spatial variability in cloud cover both along- and across-wind directions, (ii) updated estimates of narrow-FOV CF and wide-FOV FSC, (iii) updated narrow-FOV CBH, and (iv) complementary data, such as wind speed and direction from the 915-MHz Radar Wind Profiler (RWP) data. The developed record has been used successfully to assess conventional observational estimates of cloud cover and their sensitivity to the following two factors: (i) instrument-dependent cloud detection and data merging criteria and (ii) FOV configuration.

- Fourth, co-variability of the ShCu macrophysical properties and environmental parameters has been analyzed for a 3-yr period (2016-2018). Our initial analysis includes diurnal changes of FSCs obtained for clouds with small, moderate and large CEDs and several environmental parameters, such as lifted condensation level (LCL) and mixed layer height (*zi*). Preliminary results of our analysis suggest that the horizontal extent of ShCu is controlled substantially by the sign and magnitude of difference between these two parameters (*zi*-LCL): the CED tends to grow with increase of this difference (*zi* exceeds LCL).

We have initiated relationships between the ShCu and key atmospheric parameters that control both the development and evolution of ShCu using our new data product, which combines effectively the advantages of narrow-FOV data offered by zenith pointing cloud radars and lidars and wide-FOV TSI images. While the latest instrumentation at the ARM sites may address these challenging relationships in the future, we believe that the historical ARM data at the SGP site has not yet been fully utilized. Overall, our data product can be used by researchers working on a wide range of climate-related projects. These projects may include (i) a comprehensive evaluation of outputs from the Large-Eddy Simulation (LES) and single-column models for their future improvement, (ii) the representativeness of "short-period" results obtained from the previous model and observational studies and (iii) the planning of future field campaigns with focus on improved understanding of the diurnal cycle of cumulus convection.

1. Overview

Shallow cumuli (ShCu) have a number of important roles in the Earth's climate system due to their complex interactions with radiation, atmosphere and surface. The strong spatial and temporal variability of ShCu has been a topic of increasing interest in recent years for both observational and model studies. Efforts to improve model parameterizations of fair-weather ShCu utilize the cloud horizontal extent, vertical structure, and liquid water content within a model grid cell; however, corresponding observations are commonly zenith pointing with a very narrow field of view (FOV). Therefore, the cloud properties provided by these observations may not be representative of a larger surrounding area. As a result, difficulties may ensue when model outputs (for a given area) and "narrow-FOV" products (for a given point) are compared.

Our project (grant DE-SC0016084) has been focused on development of a new much-needed "wide-FOV" cloud product for the comprehensive evaluation of Large-Eddy Simulation (LES) outputs as part of the LES ARM Symbiotic Simulation and Observation (LASSO) project and Holistic Interactions of Shallow Clouds, Aerosols, and Land-Ecosystems (HI-SCALE) campaign at the Atmospheric Radiation Measurement (ARM) Southern Great Plains (SGP) 'megasite'. In particular, our project has integrated the advantages of wide-FOV passive sky imaging and narrow-FOV active remote sensing with a focus on single-layer ShCu, which are challenging to represent correctly in climate models and difficult to observe holistically.

There are four major accomplishments of our project:

1. Evaluation of an updated cloud classification to identify days with single-layer ShCu.
2. Development of a new approach to resolve cloud area distributions for a given region (up to 4x4 km^2) and determination of cloud equivalent diameters (CEDs).
3. Construction of an 18-yr (2000-2017) record of ShCu macrophysical properties from integrated narrow-FOV and wide-FOV observations. Application of the constructed record to assess two conventional measurement-based estimates of cloud cover and their differences due to (i) sensitivity to instrument-dependent cloud detection and data merging criteria, and (ii) spatio-temporal observational configurations.
4. Analysis of the co-variability of ShCu macrophysical properties and environmental parameters for a 3-yr (2016-2018) period.

These four accomplishments are summarized in the following four sections.

1. Evaluation of the updated cloud classification

Full details about the operational cloud type VAP are documented in Lim et al. (2019). Data products are available in Shi et al. (2000).

Previous ShCu studies have identified times of ShCu cloud cover using manually intensive assessment of cloud base height (CBH), fractional sky cover (FSC), cloud fraction (CF), and mesoscale cloud patterns. The new ARM ShCu Value Added Product (VAP) identifies these times operationally. The ShCu VAP is an extension of the latest ARM cloud type VAP that uses the Active Remote Sensing of Clouds (ARSCL) cloud product to identify cloud types using cloud boundary heights (Lim et al., 2019). The ShCu VAP additionally incorporates the ceilometer CF and FSC from Total Ski Imager (TSI) data to distinguish between low cloud types and detect the onset and end-times of ShCu events. The ShCu VAP provides detailed hourly descriptions of the cloudy sky, including the presence of multiple cloud types. For example, the SGP site often exhibits overlying Cirrus that can either be intermittent or persistent throughout the day (Fig.1). The ShCu VAP identifies periods with ShCu while allowing for exclusion of multiple cloud types.

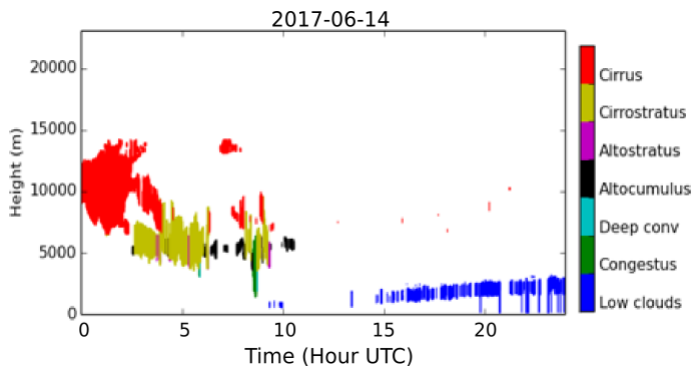

Figure 1. An example of cloud type VAP "quick-look" shows a typical period of ShCu with intermittent Cirrus at the SGP site. The ShCu VAP allows identification of periods with single-layer ShCu during which the wide-FOV products can be derived.

We have provided detailed evaluation of the ShCu VAP and shared our evaluation results with its development team. In particular, we have used the daily VAP output files to generate a dataset of periods with single-layer ShCu and compared the generated start- and end-times with those obtained from manually curated records (Berg and Kassianov, 2008; Zhang and Klein, 2013; Lamer and Kollias, 2015). Feedback from our group and other ARM users have been used by the development team to deliver the updated version of the ShCu VAP for the period of interest (2000-2017) as documented in Lim et al. (2019) and have further been incorporated into the operational version of the VAP that is being used by ARM currently. We have found that this version extends the manually curated records and provides important insight into the impact of instrumentation changes at the SGP site, namely the transition to KAZRARSCL with the updated cloud radar, on the identification of periods with single-layer ShCu.

2. Development of new "wide-FOV" cloud products

Full details about the methodology and estimation of errors and uncertainty of ShCu cloud area can be found in Kleiss et al. (2018).

Cloud horizontal size and its diurnal changes substantially influence complex surface-atmosphere interactions, including energy fluxes at the land-atmosphere boundary and the Earth's radiation budget. Although the term "cloud horizontal size" is commonly used to refer to *cloud chord length* (CCL) derived along a given direction from ground-based radar-lidar or aircraft data, model studies typically restrict the word "size" to describe the *cloud equivalent diameter* (CED) of a given cloud area. As a consequence, the data-derived CCL and model-predicted CED often cannot be compared directly especially at short temporal and spatial scales.

We have developed a novel approach that resolves cloud area distributions of single-layer ShCu from combined ground-based observations and estimates CED over a wide range of cloud sizes (about 0.01–3.5 km) with high temporal resolution (30 s). Our approach is computationally inexpensive and relies on sky images obtained from TSI data and complementary information on CBH provided by lidar measurements. We have illustrated performance of our approach using coincident 0.03-km Landsat cloud masks obtained for five periods with single-layer ShCu over the ARM SGP site.

The error and uncertainty of the CED product have been characterized by comparison with co-located and coincident high resolution (0.03 km) Landsat cloud images, as visualized in Figure 2. We have demonstrated a good (7%) agreement with Landsat cloud boundaries when (i) the total FSC is below 0.4, and (ii) clouds are within the TSI image area (~ twice the CBH). Large clouds that extend beyond the TSI image area are responsible for a noticeable (~16%) underestimation of the TSI characteristic cloud horizontal size. Our approach provides previously unavailable datasets that can contribute to improved understanding of cumulus convection at various temporal and spatial scales.

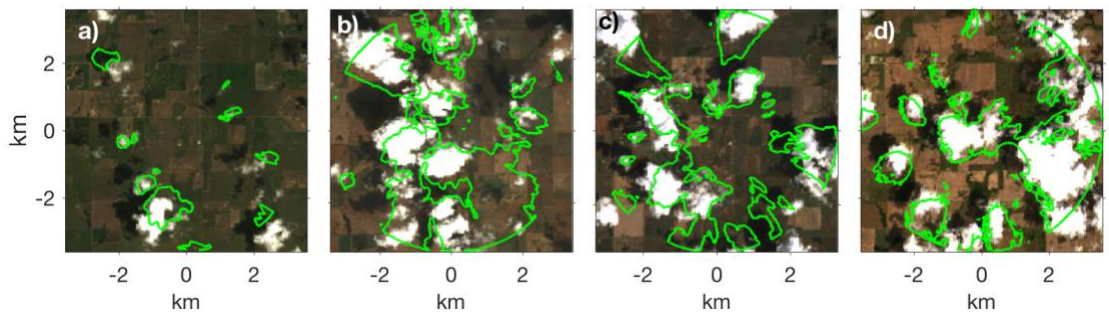

Figure 2. Co-located Landsat images comprise the validation data set for the CED calculation based on TSI images. Sample images are captured on (**a**) 2007/07/21 17:01 (**b**) 2007/09/23 17:00; (**c**) 2009/05/23 16:55; (**d**) 2017/06/14 17:06 UTC. North is up, East is right. Green lines show perimeters of cloud boundaries from the CED analysis. (**b**) Illustrates erroneous cloud boundary in the southeast quadrant due to sun glare around the TSI shadowband.

3. Development of the multi-year record of ShCu properties

Full details of the methodology and estimation of error and uncertainty of the long-term data set produced can be found in Riley et al. (2020). Data products are available in Riley et al. (2019).

We have developed two integrated records of ShCu macrophysical properties: (1) a record that spans the entire TSI record (2000-2017) with essential cloud properties and environmental conditions (Riley et al. 2019), and (2) a more intensive record covering the LASSO project and HI-SCALE campaign (2016-2018) that includes additional cloud macrophysical properties and environmental variables. This section summarizes our work and key insights from the entire (2000-2017) record; the enhanced record (2016-2018) is summarized in Section 4.

We have identified the ShCu events using a consistent approach based on the new ShCu VAP (Section 1) spanning the entire TSI record (2000-2017) of daytime hours during summer months (May-Sept). The extended record included multiple instrumental upgrades and underwent rigorous assessment of data quality. Our new data product represents the longest available compilation of events with single-layer ShCu at the SGP site and includes (i) new characterization of cross-wind variability of FSC from wide-FOV TSI observations, (ii) updated macrophysical properties from narrow FOV observations, such as CBH CF, and (iii) complementary data such as wind speed and direction from the 915-MHz Radar Wind Profiler. This record was used to examine the long-term bias and variability of cloud cover from different co-located instruments.

There are two conventional measurement-based estimates of cloud cover: (1) cloud fraction (CF) obtained from zenith-pointing narrow-FOV observations and defined as the fraction of time when a cloud is detected within a specified period and (2) fractional sky coverage (FSC) obtained from wide-FOV observations and defined as the fraction of

cloudy pixels in a sky image. Differences between CF and FSC are typically attributed to two main factors: (i) the different sensitivity to cloud properties, and (ii) different FOV configurations of the active and passive ground-based instruments. To assess the relative impact of these two main factors on ShCu cloud amount, we have divided the extended record period (2000-2017 summers) into two sub-periods (2000-2010 and 2011-2017 summers) that mark instrumentation upgrades and corresponding improvements in data merging. Our analysis has considered two guiding questions:

1. *Have significant changes in the observations of ShCu cover occurred at the SGP site due to instrumental and algorithmic upgrades?*

   We have demonstrated that the best agreement occurs between the CF obtained from the ceilometer alone and FSC obtained from TSI data for the entire period and two sub-periods. In contrast, the CF calculated from combined ceilometer and Micro Pulse Lidar (MPL) data has the largest disagreement with FSC in the first sub-period, with improvement in the second sub-period. This improvement is likely associated with updates to the MPL cloud mask, and improved merging strategies that rely more on the ceilometer data. When incorporating a threshold on the CTH, the CF obtained from the combined lidar-radar data has moderate disagreement with FSC in the first sub-period, and good agreement in the second sub-period (Fig. 3). The strong period dependence of CF obtained from the combined lidar-radar data is likely due to changes in instrumental cloud detection, with the second sub-period showing evidence of compensating errors.

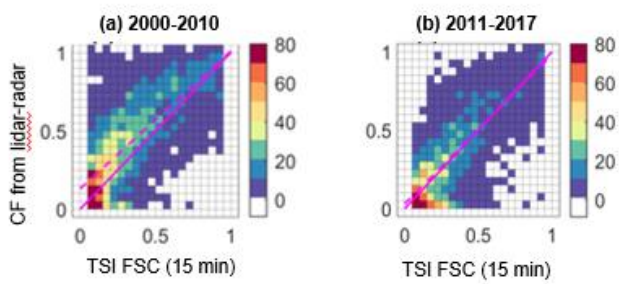

Figure 3. 2D joint histograms compare the narrow-FOV CF from the merged lidar-radar product versus the wide-FOV FSC from the TSI for two sub-periods, (a) 2000-2010, and (b) 2011-2017. Color indicates number of observations. For the first sub-period, the lidar-radar CF overestimates, on average, the FSC by 0.08, with a root mean squared difference (RMSD) of 0.18. For the second period, there is no bias between the lidar-radar CF and TSI FSC, the corresponding RMSD is 0.14.

2. *What is the impact of FOV configurations on hourly and sub-hourly observations of ShCu cover?*

   We have simulated a narrow-FOV CF-like observation from the TSI data with the instrumental sensitivity like the TSI, but spatio-temporal sampling strategy like the lidar-radar CF. This allows us to investigate the relative impacts of (1) instrumental cloud detection differences, (2) FOV configurations and (3) sampling differences on the ShCu cover estimates. We have demonstrated that the wide-FOV and narrow- FOV configurations provide, on average, comparable estimates of cloud cover for two temporal averaging windows (hourly and sub-hourly). However, the corresponding root mean squared difference (RMSD) depends upon the temporal averaging window. For hourly observations, 77% of observations agreed to within ±0.1, while for 30-min observations, 59% of observations agreed to within 0.1. Thus, narrow-FOV and wide-FOV observations introduce observational variability for shorter (sub-hourly) time periods.

This considerable impact of the FOV configuration on sub-hourly observations of ShCu, confounded with instrumental detection differences motivates the introduction of a new "quick-look" tool (Fig. 4). The “quick-look” tool uses a spatially resolved analysis of the cross-wind variability in cloud cover within the TSI 100° FOV to provide an expected range of cloud cover that would be detected by a set of 21 narrow-FOV instruments with the same detection properties as the TSI. The “quick-look” tool can identify (a) impacts of the FOV configuration on the cloud

cover estimates, (b) periods with organized cloud fields, (c) potential issues associated with data merging and cloud detection, and (d) periods with TSI data quality concerns. The generated "quick looks" and all supporting data are publicly available (Riley et al. 2019b, tsiQLtable, DOI: 10.5439/1491245).

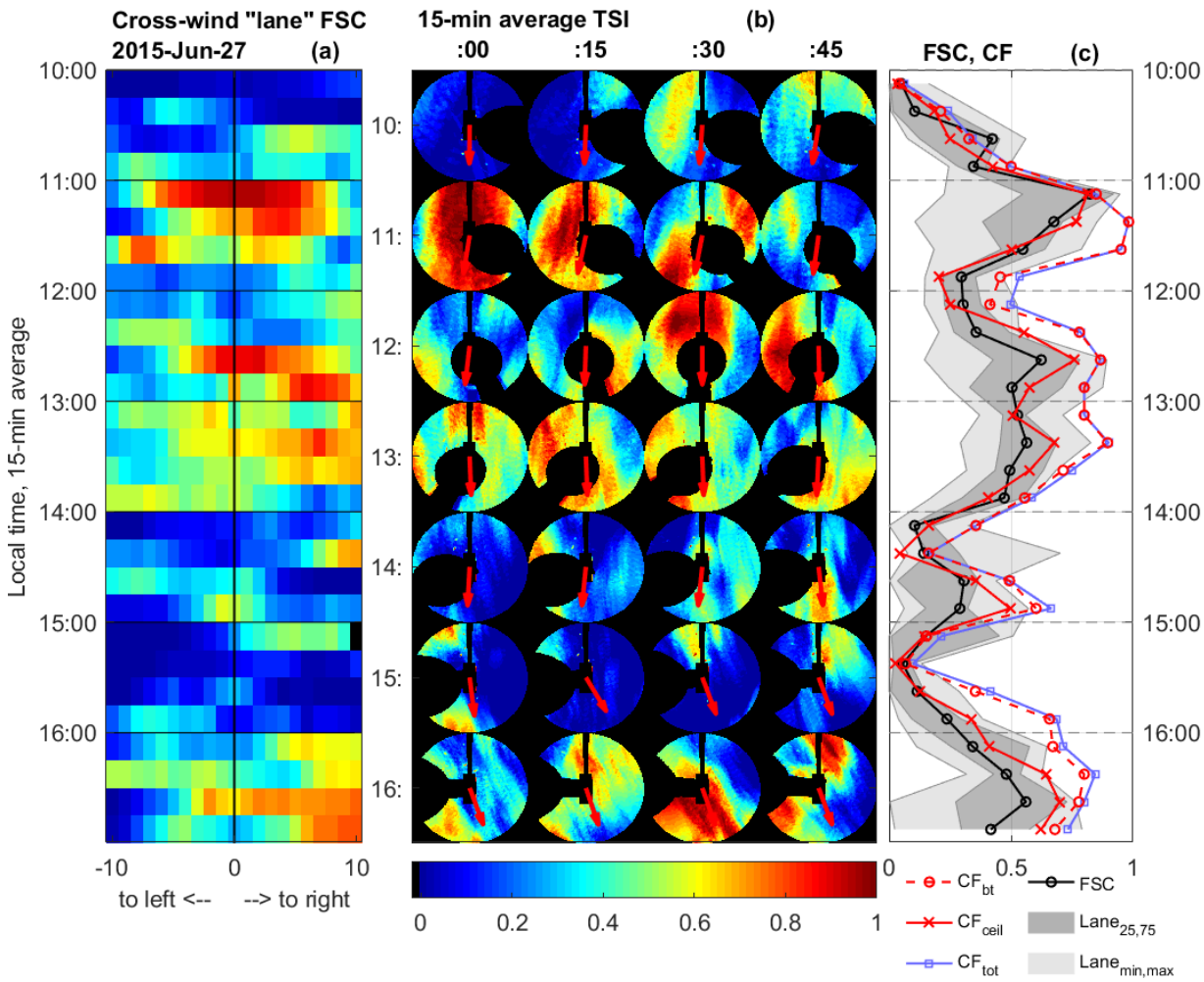

Figure 4. Example of the generated "quick look" shows FSC and CF for a given day (17 June, 2016). (a) Heat map of 15-min average CF indicated by the color bar for 21 cross-wind bins. Time runs from top to bottom; the vertical line at "0" indicates the image center along the direction of the wind. (b) 15-min composite images within the 100˚ FOV, projected onto rectilinear grid. Red arrows indicate wind direction at CBH. (c) Comparison of cloud amounts obtained from TSI and lidar-radar data: 30-min averages of CF_{bt} (CF "cloud bases and tops") from merged lidar-radar for ShCu only (red dashed with circles), CF_{ceil} (CF "from ceilometer", red line with "x" symbol), and CF_{tot} (CF "total") from merged ceilometer-MPL for any cloud detection (blue line with squares). 15-min average FSC from TSI data (black line with circles), 15-min minimum and maximum lane-averaged CF (light grey shading) and interquartile lane CF (dark grey shading). Markers are placed at time bin center.

For example, Figure 4 illustrates organized cloud fields at roughly 11:00 and 12:30 local time, with enhanced cloud coverage at zenith. The larger CF during these times may be due the narrow-FOV observation falling in a cloud street. However, the larger CF from 13:00-14:00 and after 16:00 is more likely due to instrumental detection differences. The close agreement of CF_{tot} (blue) and CF_{bt} (red circles) indicates the lack of overlying Cirrus clouds. TSI data quality concerns are not apparent.

The developed dataset provides a unique opportunity to (1) contrast the long-term cloud cover estimates with different instrumental sensitivities and data merging strategies and (2) describe the across-wind variability of cloud cover at user-specified temporal and spatial scales. These data provide an observational foundation for a better interpretation of quandaries, such as model-to-data discrepancy of cloud cover.

4. Co-variability of ShCu macrophysical properties with environmental parameters.

A manuscript documenting this work is in preparation (Kleiss et al., 2020).

An enhanced record has been developed for the recent period (2016-2018) that includes the LASSO project and HI-SCALE campaign. This record builds upon the long-term record (Section 3), and includes (i) FSC partitioned by cloud horizontal size (ii) additional environmental variables including boundary layer stability, soil moisture, surface fluxes, and mixed layer height. This is the first temporally and spatially dense record of FSC partitioned by cloud horizontal size.

We have used this record to assess the ShCu onset and CED evolution related to local environmental conditions. Cloud vertical extent may be related to boundary layer height, relative humidity, updraft velocity, environmental lapse rate, and inversion capping strength. Less is known about environmental impact on cloud horizontal size. This impact can be characterized by several environmental parameters, such as lifted condensation level (LCL) and mixed layer height (*zi*). Hereafter, their normalized difference (LCL-*zi*)/LCL, is referred to as "environmental overlap".

To estimate a statistical relationship between the measurement-based "environmental overlap" and the CED, we have applied a four-step approach. First, we have calculated CED following the methodology of Kleiss et al. (2018). Recall, clouds with large horizontal size (CED > 2CBH) may not be fully resolved due to possible extension beyond the TSI FOV (Kleiss et al., 2018). Second, we have segregated the observed clouds into four groups using the calculated CED as follows:

- Small: CED/LCL < 0.75
- Medium: 0.75 < CED/LCL < 1.5
- Large: 1 < CED/LCL < 2
- Non-resolvable: 2 < CED/LCL

Third, we have computed half-hour averages of CED-resolved FSC on a rolling 10-min basis. Note, the sum of the CED-resolved FSCs calculated for clouds with small, medium, large, and non-resolvable CED is the total FSC. The corresponding half-hour averages of "environmental overlap" have been computed from the surface temperature and humidity (for LCL) and doppler lidar vertical variance (for *zi*). Finally, we have performed a statistical analysis to demonstrate a strong co-variability of the "environmental overlap" and the CED (Fig. 5). For example, the peak of the probability distribution function of the "environmental overlap" is shifted from small positive values to moderate negative values when the CED increases from small to non-resolvable values (Fig. 5a). As far as we aware, this is the first successful demonstration of such relationship, which can be beneficial for a comprehensive evaluation of the existing and future ShCu parameterizations.

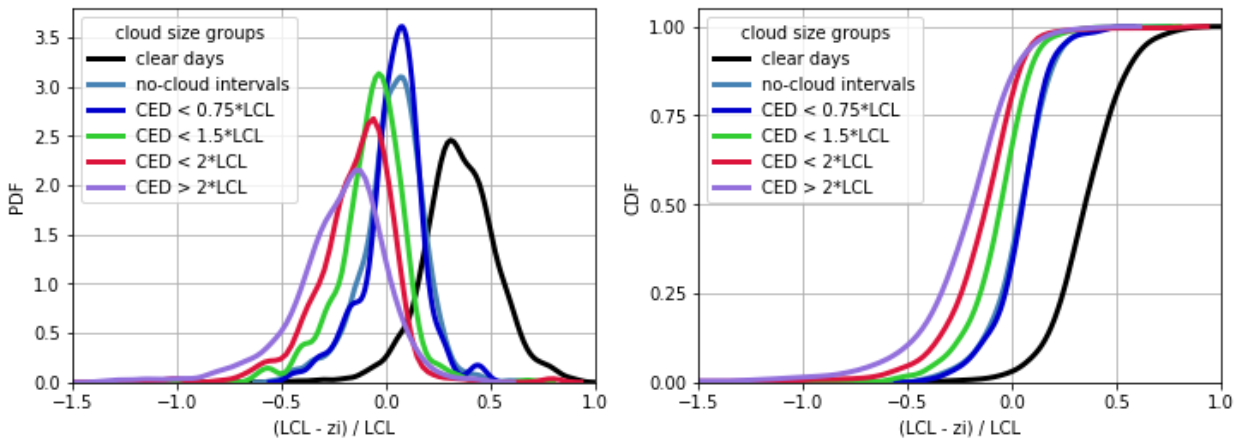

Figure 5. Probability density function (PDF) and cumulative distribution function (CDF) of the 30-min "environmental overlap" observed for cloud fields composed of clouds with different CEDs. All observations are half-hour averages (rolling every 10 minutes) obtained during 3-year (2016-2018) period. Black: Clear-sky days without ShCu events (N = 1825). Gray: half-hour "no clouds" periods that are observed within ShCu events (N = 1296). Blue: All observed clouds are in the "small" category (N = 389). Green: All periods have "medium" clouds and smaller (N = 866). Red: All periods contain "large" clouds and smaller (N = 462). Purple: All periods contain "non-resolved" (clouds with CED > 2 x LCL) and smaller (N = 818).

Overall, our data product can be used by researchers working on a wide range of climate-related projects. These projects may include (i) a comprehensive evaluation of the outputs from the LES and single-column models for their future improvement, (ii) the representativeness of "short-period" results obtained from the previous model and observational studies and (iii) the planning of future field campaigns with focus on improved understanding of the diurnal cycle of cumulus convection.

References:

Kleiss, J. M., Riley, E. A., Long, C. N., Riihimaki, L. D., Berg, L. K., Morris, V. R. and Kassianov, E.: Cloud Area Distributions of Shallow Cumuli: A New Method for Ground-Based Images, *Atmosphere*, 9(7), 258, https://doi.org/10.3390/atmos9070258, 2018.

Kleiss, J. M., Riley E. A., Barton, K., Riihimaki L.D., Berg L.K., and Kassianov E.: Environmental Controls of Shallow Cumulus Horizonal Size, *in preparation*. 2020

Lim, S. K., Riihimaki, L. D., Shi, Y., Flynn, D., Kleiss, J. M., Berg, L. K., Gustafson Jr., W. I., Zhang, Y., and. Johnson, K. L.: Long-Term Retrievals of Cloud Type and Fair-Weather Shallow Cumulus Events at the ARM SGP Site, *Journal of Atmospheric and Oceanic Technology*, 36, 2031–2043, https://doi.org/10.1175/JTECHD-18-0215.1, 2019.

Riley, E. A., Kleiss, J. M., Riihimaki, L. D., Long, C. N., Berg, L. K. and Kassianov, E.: Shallow Cumuli Cover and Its Uncertainties from Ground-based Lidar-Radar Data and Sky Images, *Atmospheric Measurement Techniques*, 1–30, https://doi.org/10.5194/amt-13-2099-2020, 2020.

Riley E. A., Kleiss J. M., Riihimaki L.D., Long C.N., Berg L.K., and Kassianov E.: TSI composite images merged cloud fraction product for shallow cumulus cases (tsiQLtable) 2000-2017. http://dx.doi.org/10.5439/1491245, 2019.

Shi, Y., Flynn, D., and Riihimaki, L.: Fair-Weather Shallow Cumulus Identification (SHALLOWCUMULUS) at Southern Great Plains (SGP) Central Facility, Lamont, OK (C1), Atmospheric Radiation Measurement (ARM) user facility, Oak Ridge, Tennessee, USA, https://doi.org/10.5439/1392569, 2000.

Published conference proceedings

Kassianov, E., Riley, E. A., Kleiss, J. M., Long, C. N., Riihimaki, L., Flynn, D., Flynn, C. and Berg, L. K.: Macrophysical properties of continental cumulus clouds from active and passive remote sensing, *Proceedings SPIE 10424, Remote Sensing of Clouds and the Atmosphere XXII*, 104240A, https://doi.org/10.1117/12.2278029, 2017.

Kassianov, E., Riley, E. A., Kleiss, J. M., Riihimaki, L., Long, C. N., Morris, V. and Berg, L. K.: Shallow cumulus macrophysical properties at midcontinental US site: integrated multiyear active and passive observations, *Proceedings SPIE 10786, Remote Sensing of Clouds and the Atmosphere XXIII*, 107860O, https://doi.org/10.1117/12.2326691, 2018.

Kassianov, E., Riley, E. A., Kleiss, J. M., Riihimaki, L. and Berg, L. K.: Macrophysical properties of continental shallow cumuli: diurnal evolution, *Proceedings SPIE 11152, Remote Sensing of Clouds and the Atmosphere XXIV*, 111520A, http://dx.doi.org/10.1117/12.2534359, 2019.

Related presentations listed chronologically

Riley, E., Kleiss J.M., Long, C. N., Riihimaki L., Berg L., and Kassianov E.: Macro-physical Properties of Shallow Cumulus from Integrated ARM Observations: Development of a New Data Product for Model Evaluation. Poster at *Atmospheric System Research / Atmospheric Radiation Measurement PI meeting*, Washington D.C. 2017.

Kleiss, J., Riley, E., Kassianov, E., Long, C., Riihimaki, L., and Berg, L.: Macro-physical Properties of Shallow Cumulus Clouds at the ARM SGP Site: Enhanced Ground-Based Observations from the Total Sky Imager. Poster at *American Geophysical Union Annual Meeting*, New Orleans, LA. 2017.

Riley, E.A., Kleiss J.M., Long, C. N., Riihimaki L., Berg L.K., and Kassianov E.: The Influence of Cloud Field Uniformity on Observed Cloud Amount. Poster at *American Geophysical Union Fall Meeting*, New Orleans, Louisiana. 2017.

Kleiss, J., Riley, E., Long, C., Riihimaki, L., Berg, L., Morris, V., and Kassianov, E.: Macro-physical Properties of Shallow Cumulus Clouds at the ARM SGP Site: Enhanced Ground-Based Observations from the Total Sky Imager. Poster and Plenary Talk at *Atmospheric System Research / Atmospheric Radiation Measurement PI meeting*, Washington D.C. 2018.

Kleiss, J., Riley, E., Long, C., Riihimaki, L., Berg, L., Morris, V., and Kassianov, E.: Shallow Cumuli at the SGP Site: Macrophysical and Environmental Properties. Poster at *Atmospheric System Research / Atmospheric Radiation Measurement PI meeting*, Washington D.C. 2019.

Riihimaki, L.D.: Using multi-instrument observations of shallow cumulus as a tool for improving simulations of cloud radiative impacts. Invited talk at *NOAA ESRL Global Monitoring Division Seminar*. 2019.